Excimer and Electromer Suppression of Tetraphenylsilane-Based Blue-Light-Emitting Polymers

Rong-Ho Lee, Ying-Yu Wang

Department of Chemical Engineering, National Yunlin University of Science & Technology, Yunlin 640, Taiwan, Republic of China

Received 19 March 2007; accepted 15 September 2007
DOI 10.1002/app.27417
Published online 3 December 2007 in Wiley InterScience (www.interscience.wiley.com).

ABSTRACT: Excimer and electromer suppression of tetraphenylsilane-derivative-based blue polymer light-emitting devices (PLEDs) was investigated. Tetraphenylsilane with a rigid bulky structure certainly but not completely suppressed excimer formation among polymer-chain segments. A poor solvent, toluene, resulted in excimer formation in the solid film during the spin-coating process, which could not be suppressed by the incorporation of a bulky moiety onto the polymer backbone. In addition, electromers or electroplexes formed by the strong interaction between the oxadiazole and diphenyl(4-tolyl)-amine groups could not be prevented by the tetraphenylsilane moiety. The influences of the bulky moiety, bipolar unit, and device fabrication conditions on the suppression of excimers or electromers in PLEDs are discussed in detail. © 2007 Wiley Periodicals, Inc. J Appl Polym Sci 107: 3459–3468, 2008

Key words: conjugated polymers; light-emitting diodes (LED); luminescence

INTRODUCTION

Polymer light-emitting devices (PLEDs) have been the focus of recent, extensive research. Their low turn-on voltage, high brightness, high efficiency, easy processing, and low-cost fabrication give them commercialization potential in the flat-panel display market.[1,2] Alkylfluorene copolymers have proven to be the most promising because of their combined desired properties, including a high fluorescence quantum yield and good film-forming and hole-transporting properties.[3–6] However, polyalkylfluorene (PF) application in PLEDs has been hampered because of undesired long-wavelength excimer emission band formation.[7–16] Excimer emission from aggregates formed by polymer-chain π–π stacking in PFs usually results in lower efficiency and a light emission redshift from blue to blue green.[7–16] Resolving the polymer-chain aggregation problem in terms of the development of light-emitting polymers (LEPs) with excellent electroluminescence (EL) properties is, therefore, important.

Various strategies have been adopted for reducing PF aggregation formation to obtain PLEDs with excellent EL performances. The aggregation and excimer effects of PFs could be suppressed by either the incorporation of bulky or branch side-chain substituents onto a polymer backbone or by blending with a high-glass-transition-temperature (T_g) conjugated polymer to reduce interaction between polymer chains.[7–12] The incorporation of polyhedral oligomeric silsesquioxane onto the polymer backbone could also improve PF's thermal stability and EL performance.[13–16] Significantly enhanced EL characteristics have been attributed to reduced aggregation and excimer formation or lower keto defects.[13–16] Recently, a series of tetraphenylsilane-based hyperbranched blue-light-emitting alkylfluorene copolymers were developed by He and coworkers.[17–19] No excimer formation in longer wavelength like emissions at 500–600 nm was observed for such hyperbranched PFs. The color purity of blue emissions was shown to be improved by the reduction of the aggregates formed by polymer-chain π–π stacking in the solid state of PFs. However, the presence of the tetrahedral molecular skeleton of tetraphenylsilane groups or the hyperbranched structure effect on the reduced aggregation and excimer formation of PF were not clarified.[17–19] More recently, a comparative study on light-emitting copolymers of fluorene and carbazole with a full conjugated or Si-interrupted structure was carried out by He et al.[20] The results seem to conclude that the self-aggregation of PF could be significantly reduced because of the steric effect of the tetrahedral molecular skeleton of teterphenylsilane groups. In fact, the maximum and full width at half-maximum (fwhm) of the emissions

Correspondence to: R.-H. Lee (lerongho@yuntech.edu.tw).
Contract grant sponsor: National Science Council of Taiwan, Republic of China; contract grant number: NSC 94-2216-E-224-005.

Journal of Applied Polymer Science, Vol. 107, 3459–3468 (2008)

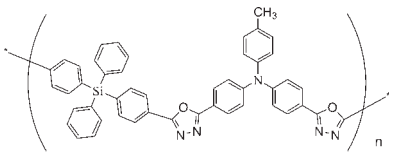

Figure 1 Chemical structure of the LEP PTOA.

were not reduced as the conjugated structure was interrupted by the teterphenylsilane group.[20] Apart from that, the tetrahedral molecular skeleton effect on the optical properties of bipolar-emitter-based LEP has not been thoroughly examined. Both steric structure and solvatochromic effects play important roles in affecting PF aggregation and excimer formation of PLEDs. It is important to learn which effect exerts more influence.

To investigate the steric structure effect on the reduction of PF aggregation and excimer formation, two tetraphenylsilane–fluorene–diphenyl(*para*-toyl)-amine polymers, PTFA1 and PTFA2, containing 25 and 50 mol % of tetraphenylsilane groups, respectively, were synthesized. Moreover, a tetraphenylsilane–oxadiazole–diphenyl(*para*-tolyl)amine polymer (PTOA), containing a bipolar emitter moiety (e.g., triarylaminooxadiazole), was also synthesized for the sake of comparison.[21] The chemical structure of PTOA is shown in Figure 1. The ultraviolet–visible (UV–vis) absorption, photoluminescence (PL) emission, EL emission, and EL performances of PTFA1 and PTFA2 were studied in comparison with those of poly[2,7-(9,9)-dioctylfluorene] (PFO), poly[9,9-dioctylfluorene-*co*-*N*-(4-methylphenyl)diphenyl-amine] (PFA), and PTOA. Correlations between the molecular structure, optical properties, and EL properties of the tetraphenylsilane-based LEPs are discussed in detail. In addition, the optoelectronic properties of PTFA1- and PTFA2-based light-emitting layers coated with cyclohexanone and toluene solutions, respectively, were also investigated. These properties are compared with the structure effect on the suppression of excimer formation among the polymer chains.

EXPERIMENTAL

LEP synthesis

All reactions and manipulations were performed in a nitrogen atmosphere with standard Schlenk techniques. All chromatographic separations were carried out on silica gel. *O*-Xylene, diethyl ether, and anisole were distilled over sodium/benzophenone in a nitrogen atmosphere. Dimethylformamide was dried over $CaSO_4$. Chemicals were reagent grade and purchased from Aldrich (St. Louis, MO), Fluka (Buchs SG, Switzerland), Sigma, and RDH Chemical Co. PTOA was synthesized according to the literature.[21] PFO and PFA were synthesized according to the literature by a Suzuki coupling reaction.[3] The preparation of PTOA was reported in our previous article.[21] Schemes 1–3 illustrate the synthetic route for the preparation of PFO, PFA, and the PTFAs. Detailed synthesis procedures are reported next.

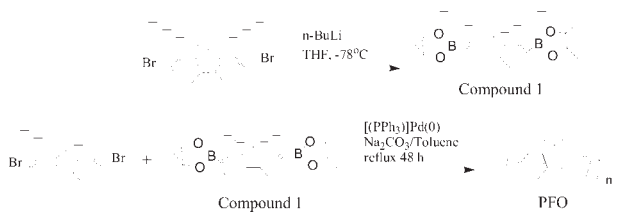

Scheme 1 Synthesis of the LEP PFO.

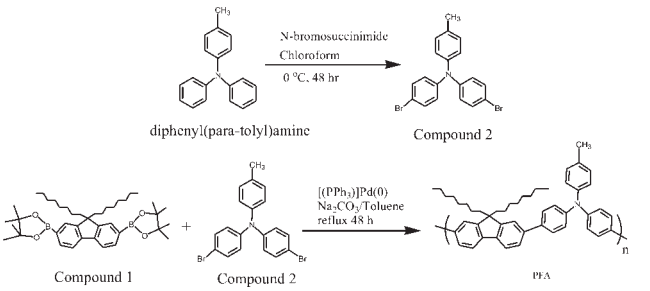

Scheme 2 Synthesis of the LEP PFA.

Synthesis of 2,7-bis(4,4,5,5-tetramethyl-1,3, 2-dioxaborolan-2-yl)-9,9-dioctylfluorene (compound **1**)

Compound **1** was synthesized according to the literature.[3] The white solid product yield was 60.0%.

^{1}H-NMR (600 MHz, $CDCl_3$, δ, ppm): 7.80–7.81 (d, 2H, J = 7.8 Hz), 7.74 (s, 2H), 7.71–7.73 (d, 2H, J = 7.2 Hz), 1.98–2.02 (m, 4H), 1.4 (s, 24H), 1.2 (m, 4H), 0.99–1.12 (m, 16H), 0.81 (t, J = 14.4 Hz, 6H),

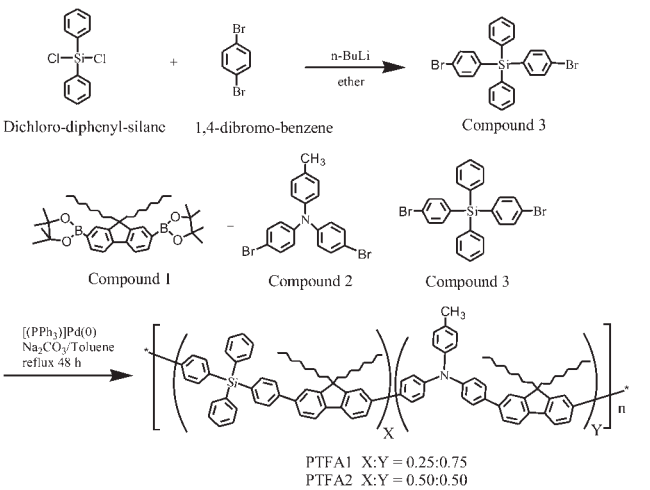

Scheme 3 Synthesis of the LEPs PTFA1 and PTFA2.

0.58 (m, 4H). ANAL. Calcd for $C_{41}H_{64}B_2O_4$: C, 76.56%; H, 9.96%; N, 0%. Found: C, 76.43%; H, 9.13%; N, 0%.

Polymerization of PFO

PFO was synthesized according to a procedure from the literature via a Suzuki coupling reaction of 2,7-dibromo-9,9-dioctylfluorene and compound **1.**[3] The brown solid product yield was 72.8%. The number- and weight-average molecular weights of PFO measured by gel permeation chromatography (GPC) were about 18,437 and 31,855 g/mol.

^{1}H-NMR (600 MHz, $CDCl_3$, δ, ppm):7.83 (d, 2H, J = 25.8 Hz), 7.69 (s, 2H), 7.68 (d, 2H, J = 24 Hz), 1.959–2.12 (t, J = 39 Hz, 4H), 1.09–1.25 (m, 20H), 0.72–0.89 (m, 6H), 0.58 (m, 4H). ANAL. Calcd for $C_{29}H_{40}$: C, 89.55%; H, 10.29%; N, 0%. Found: C, 89.44%; H, 9.08%; N, 0%.

Synthesis of (4,4′-dibromo-4″-methyl)triphenylamine (compound **2**)

N-bromosuccinimide (1.9569 g, 11 mmol) was added dropwise to a chloroform (20-mL) solution containing diphenyl-*p*-tolyl-amine (1.2965 g, 5 mmol) at 0°C in a nitrogen atmosphere. The reaction mixture was reacted for 48 h, then quenched with water, and extracted with ethyl acetate. The organic layer was dried over anhydrous magnesium sulfate followed by solvent evaporation in a rotary evaporator. A solid crude product was recrystallized in hexane–methanol to afford a white solid product. The white solid product yield was 74.0% (1.54 g).

^{1}H-NMR (600 MHz, $CDCl_3$, δ, ppm): 7.295 (d, J = 9.6 Hz, 4H), 7.071 (d, J = 7.8 Hz, 2H), 6.948 (d, J = 8.4 Hz, 2H), 6.893 (d, J = 9 Hz, 4H), 2.304 (s, 3H). ANAL. Calcd for $C_{19}H_{15}Br_2N$: C, 54.66%; H, 3.6%; N, 3.36%. Found: C, 54.91%; H, 4.01%; N, 3.2%.

Polymerization of PFA

PFA was synthesized according to a procedure from the literature via a Suzuki coupling reaction of compounds **1** and **2**.[3] The brown solid product yield was 76.4%. The number- and weight-average molecular weights of PFA, as measured by GPC, were about 18,125 and 32,444 g/mol, respectively.

^{1}H-NMR (600 MHz, $CDCl_3$, δ, ppm): 7.74–7.77 (d, 2H), 7.54–7.59 (m, 4H), 7.22–7.26 (m, 6H), 7.06–7.14 (m, 6H), 2.36 (s, 3H), 2.02 (t, 4H, J = 7.8 Hz,), 1.76 (m, 4H), 1.06–1.20 (m, 20H), 0.72–0.81 (t, 6H, J = 51 Hz), 0.7(m, 4H). ANAL. Calcd for $C_{48}H_{55}N$: C, 89.17%; H, 8.51%; N, 2.17%. Found: C, 86.6%; H, 8.71%; N, 1.89%.

Synthesis of (4-4′-dibromophenyl) diphenylsilane (compound **3**)

n-Butyllithium (1.6*M*, 22.5 mL, 36 mmol) was added dropwise to a dry ether solution (60 mL) containing 1,4-dibromo-benzene (9.4368 g, 40 mmol) under a nitrogen atmosphere at −78°C. The reaction solution was further stirred for 2 h. Dichloro-diphenyl-silane (5.064 g, 20 mmol) was then added dropwise to the solution. The solution was stirred and gradually allowed to warm to room temperature over 5 h. The reaction was then quenched with water. The mixture was finally extracted with ether. The white solid product was isolated by flash-column chromatography (silica gel, with hexane as the eluent). The brown solid product yield was 32.0% (3.17 g).

^{1}H-NMR (600 MHz, $CDCl_3$, δ, ppm): 7.49–7.51 (m, 8H), 7.44 (t, 2H, J = 15 Hz), 7.36–7.38 (m, 8H). ANAL. Calcd for $C_{24}H_{18}Br_2Si$: C, 58.26%; H, 3.64%; N, 0%. Found: C, 58.67%; H, 3.46%; N, 0%.

Polymerization of PTFA1

Compound **1** (2.57 g, 4 mmol), compound **2** (1.67 g, 4 mmol), compound **3** (0.99 g, 2 mmol), and $Pd(PPh_3)_4$ (0.09 g, 0.078 mmol) were dissolved in a mixture of toluene and aqueous Na_2CO_3 (0.48 g in 3 mL of H_2O). The solution was refluxed with vigorous stirring under a nitrogen atmosphere for 48 h. The whole mixture was then poured into methanol (200 mL), and the precipitated material was filtered. The polymer was dissolved in a small amount of tetrahydrofuran (THF) and precipitated into methanol several times. The purified polymer was filtered and dried *in vacuo*. The white solid PTFA1 yield was 59.4% (1.93 g). The number- and weight-average molecular weights of PTFA1, as measured by GPC, were about 15,125 and 27,376 g/mol.

^{1}H-NMR (600 MHz, $CDCl_3$, δ, ppm): 7.53–7.79 (m, 24H), 7.37–7.50 (m, 18H), 6.98–7.26 (m, 36H), 2.34–2.45 (m, 9H), 2.01 (s, 16H), 1.04–1.25 (m, 80H), 0.74–0.82 (m, 24H), 0.66–0.74 (16H). ANAL. Calcd for $C_{149}H_{223}N_3Si$: C, 83.24%; H, 9.05%; N, 1.42%. Found: C, 83.57%; H, 10.42%; N, 1.85%.

Polymerization of PTFA2

Compound **1** (1.29 g, 2 mmol), compound **2** (0.42 g, 1 mmol), compound **3** (0.5 g, 1 mmol), and $Pd(PPh_3)_4$ (0.046 g, 0.0395 mmol) were dissolved in a mixture of toluene and aqueous Na_2CO_3 (0.48 g in 3 mL of H_2O). The reaction and purifying procedures were the same as those of PTFA1. The white solid PTFA2 yield was 53.9% (1.0563 g). The number- and weight-average molecular weights of PTFA2, as measured by GPC, were about 11,038 and 19,647 g/mol, respectively.

^{1}H-NMR (600 MHz, $CDCl_3$, δ, ppm): 7.53–7.79 (m, 24H), 7.35–7.50 (m, 10H), 6.98–7.23 (m, 8H), 2.27–2.38 (m, 3H), 2.02 (m, 8H), 1.04–1.43 (m, 40H), 0.74–0.82 (m, 12H), 0.66–0.74 (8H). ANAL. Calcd for $C_{101}H_{113}NSi$: C, 80.53%; H, 8.25%; N, 1.02%. Found: C, 80.20%; H, 7.56%; N, 0.8%.

Instruments

^{1}H-NMR spectra were recorded on a Bruker AMX 400-MHz spectrometer (Bruker AXS Inc., Madison, WI). Elemental analysis was carried out with an elemental analyzer (Elementar Vario EL III, Hanan, Germany). GPC measurements were carried out on a Waters chromatograph (Waters, 717 Plus autosampler). Two Waters Styragel linear columns were used, with polystyrene as the standard and THF as the eluent. T_g was measured by differential scanning calorimetry (DSC; TA Instruments, Wilmington, DE, DSC-2010) in a nitrogen atmosphere at a heating rate of 10°C/min. Thermogravimetric analysis (TGA) was performed in a nitrogen atmosphere at a heating rate of 10°C/min with a thermogravimetric analyzer (TA Instruments, Wilmington, DE, TGA-2050). UV–vis spectra were measured with a Hewlett-Packard 8453 instrument with a photodiode array detector. PL and EL spectra were recorded on a Hitachi F-4500 fluorescence spectrophotometer (Tokyo, Japan). The redox potentials of the polymers were determined by cyclic voltammetry with a BAS 100B electrochemical analyzer at a scanning rate of 100 mV/s. The polymer was dissolved in deoxygenated dry THF with 0.1*M* tetrabutylammonium perchlorate as the electrolyte. A platinum working electrode and a saturated nonaqueous $Ag/AgNO_3$ referenced electrode were used. Ferrocene was applied for potential calibration (all reported potentials were referenced against Ag/Ag+) and for reversibility criteria.

EL device fabrication and characterization

The PLED structure in this study was indium-tin oxide (ITO) glass/poly(3,4-ethylene dioxythiophene) (PEDOT)/LEP/Ca (10 nm)/Al (100 nm). ITO-coated glass, with a sheet resistance of 15 Ω/Sq and was purchased from Applied Film Corp. (Alzenau, Germany) Glass substrates with patterned ITO electrodes were well washed and cleaned by O_2 plasma treatment. A thin film (600 Å) of the hole-transporting material PEDOT (AI4083, Bayer, Goslar, Germany) was formed on the ITO layer of a glass substrate by the spin-casting method and dried at 120°C for 1 h. LEPs were then spin-coated from the 20 mg/mL cyclohexanone or toluene solution onto the PEDOT layer and dried at 80°C for 1 h in a glovebox. A high-purity Ca (20-nm) cathode was thermally deposited onto the LEP thin film, followed by Al metal (120 nm) deposition as the top layer, in a high-vacuum chamber. The PLED after electrode deposition was transferred from the evaporation chamber to a glovebox purged by high-purity nitrogen gas to keep oxygen and moisture levels below 1 ppm. The device was then encapsulated by glass covers sealed with UV-cured epoxy glue in the glovebox. The cathode deposition rate was determined with a quartz thickness monitor (STM-100/MF, Sycon, NY). The thin-film thickness was determined with a surface texture analysis system (3030ST, Dektak, Veeco Instrument Inc., NY). Current–voltage characteristics were measured on a programmable electrometer with current and voltage sources (Keithley 2400). Luminance was measured with a BM-8 luminance meter (Topcon, NJ).

RESULTS AND DISCUSSION

Synthesis and characterization of the LEPs

Chemical structure characterization and thermal properties of the LEPs

The chemical structures of PTFA1 and PTFA2 were characterized by ^{1}H-NMR spectroscopy. The ^{1}H-NMR spectrum of PTFA1 is shown in Figure 2(a).

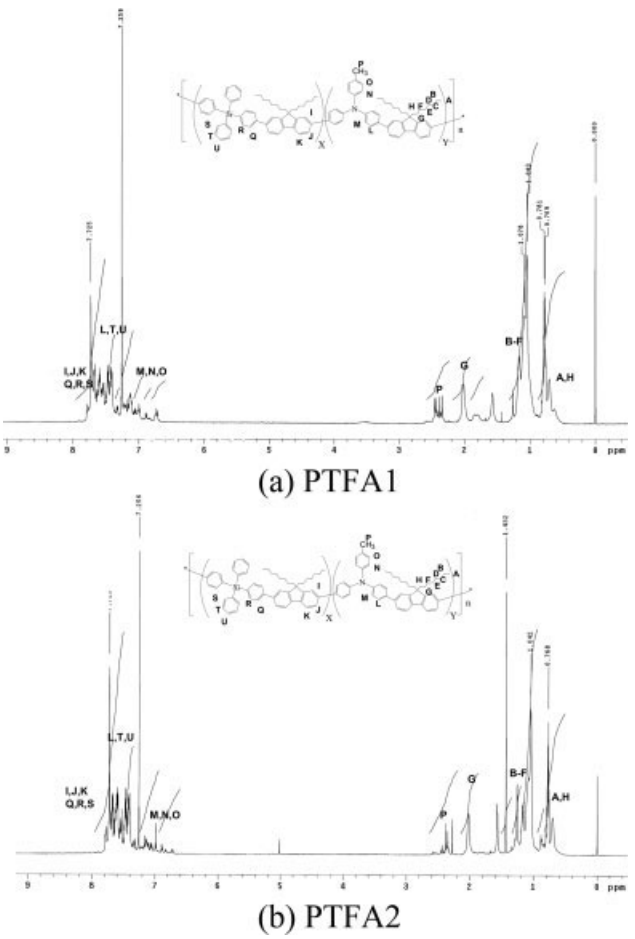

Figure 2 ^{1}H-NMR spectra of the LEPs PTFA1 and PTFA2.

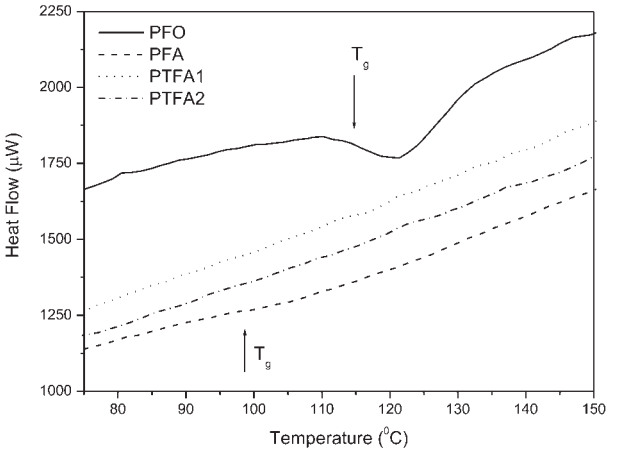

Figure 3 DSC thermograms of the LEPs.

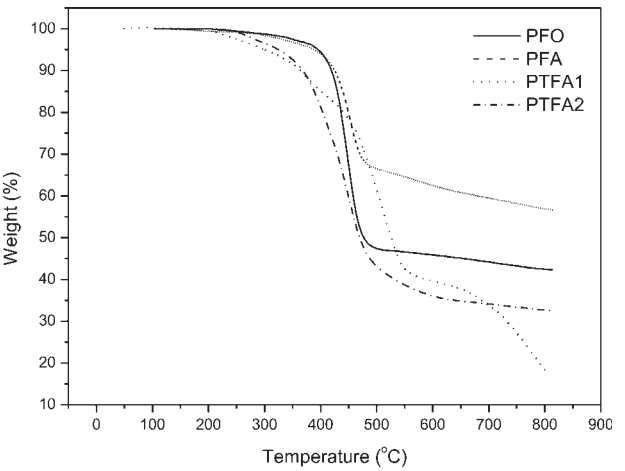

Figure 4 TGA thermograms of the LEPs.

The ^{1}H-NMR spectrum revealed that the molar ratio of the 9,9-dioctylfluorene, diphenyl(*para*-toyl)amine, and tetraphenylsilane moieties was approximately 1 : 0.75 : 0.25 for PTFA1. Additionally, the ^{1}H-NMR spectrum of PTFA2 is shown in Figure 2(b). The ^{1}H-NMR spectrum revealed that the molar ratio of the fluorine, diphenyl(*para*-toyl)amine, and tetraphenylsilane moieties was nearly 1 : 0.5 : 0.5.

The LEP thermal properties were analyzed with DSC and TGA in a nitrogen atmosphere. LEP thermal stability plays an important role in PLED operating stability. PLED operational lifetime is directly related to LEP thermal stability and T_g.[9] High T_g and degradation temperature (T_d) values are favorable for LEP application in outdoor displays. In Figure 3, the DSC thermograms show that the T_g's of PFO and PFA were at 121 and 102°C, respectively. Glass transitions were not observed for PTFA1 and PTFA2; this was attributed to the presence of rigid tetraphenylsilane groups.[21] The incorporation of the rigid tetraphenylsilane moiety in the polymer backbone would considerably reduce polymer-chain molecular mobility and, thus, reduce the enthalpy change during the glass transition for PTFA1 and PTFA2. The TGA thermograms of the LEPs are shown in Figure 4. The 5% weight loss degradation temperatures appeared at 399, 390, 308, and 329°C for PFO, PFA, PTFA1, and PTFA2, respectively. The TGA results show that PFO had the same thermal stability as PFA, whereas the T_d's of the tetraphenylsilane-containing polymers was reduced compared to that of PFA. This was because the bonding energy between the nitrogen and phenyl group in diphenyl(para-*toyl*)amine (291.6 kJ/mol) was higher than that between the silicon and phenyl groups in tetraphenylsilane (289.9 kJ/mol).[22] Although the 5% weight loss degradation temperature of PTFA2 was higher than that of PTFA1, the onset of weight loss temperature of PTFA1 was higher than that of PTFA2. This implied that the PTFA1 had a better thermal stability than PTFA2.

UV–vis absorption spectra of the LEPs

The UV–vis absorption spectra of the LEPs in solution and in the solid state are shown in Figures 5 and 6, respectively. In solution, PFO showed a maximal absorption peak at 381 nm, which was attributed to the strong featureless π–π* transition.[6] The absorption peak was slightly blueshift for PFA in comparison with PFO, which indicated the incorporation effect of the diphenyl(*para*-toyl)amine group on the electronic band gap of the polymer. Compared to that of PFA, maximal absorptions of PTFA1 and PTFA2 in cyclohexanone shifted to 342- and 345-nm wavelengths, respectively, because of the reduction of the conjugated length in the polymer backbone. With increasing tetraphenylsilane group content, the absorption intensity in the range 350–400 nm was reduced for the PTFA1 and PTFA2 samples. Absorption intensities for PTFA1 and PTFA2 in cyclohexanone decreased drastically at wavelengths

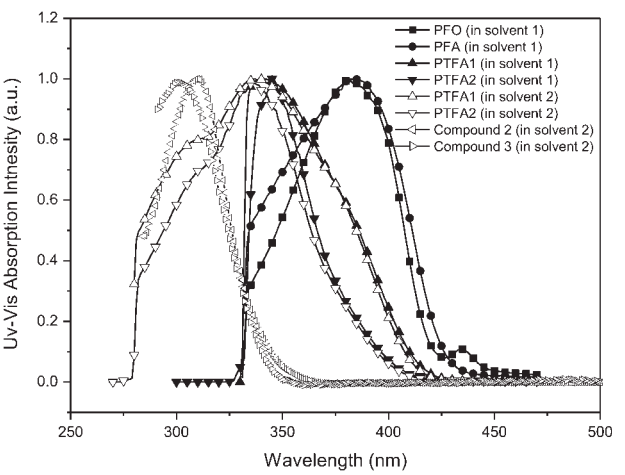

Figure 5 UV–vis absorption spectra of compounds **2** and **3** and the LEPs in different solution states [filled symbols: solvent 1 (cyclohexanone); open symbols: solvent 2 (toluene)].

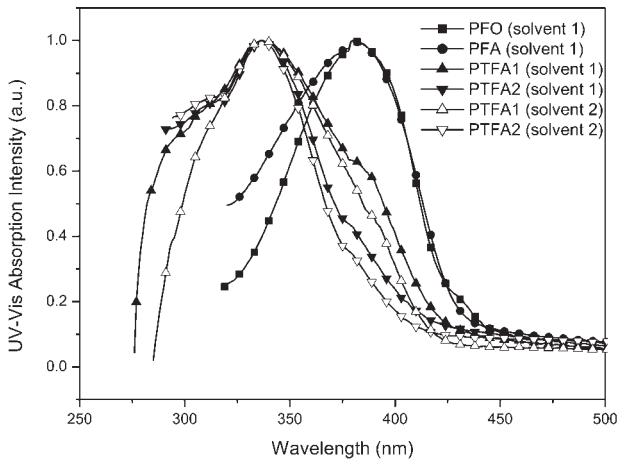

Figure 6 UV–vis spectra of the LEP solid films [filled symbols: solvent 1 (cyclohexanone); open symbols: solvent 2 (toluene)].

below 330 nm because cyclohexanone as the measuring reference absorbed radiation below 330 nm. PTFA1 and PTFA2 in toluene exhibited maximum absorptions at wavelengths of 337 and 336 nm, respectively. A 44-nm blueshift of the UV–vis absorption peaks was observed for the PTFA1 and PTFA2 samples, compared to that of PFA. This was because of the incorporation of tetraphenylsilane groups in the polymer backbone. Moreover, the presence of an absorption shoulder around 300 nm was attributed to the absorption of diphenyl(*para*-toyl)amine and tetraphenylsilane groups. As shown in Figure 5, compounds **2** and **3** in toluene showed maximum absorption peaks at wavelengths of 310 and 302 nm, respectively. As well as PFO, PFA in the solid film state showed a maximum absorption at 380 nm. No significant difference in maximum absorption wavelengths was observed in the solid film state as compared with the ones in solution. In addition, the solid thin films of PTFA1 and PTFA2 showed main absorption peaks at 340 nm, accompanied by two shoulders around 300 and 380 nm. With increasing tetraphenylsilane group content, the intensity of the absorption at the wavelength in the range 350–400 nm was reduced for the PTFA1 and PTFA2 samples. Similarly, the presence of an absorption shoulder around 300 nm was attributed to the absorption of diphenyl(*para*-toyl)amine and tetraphenylsilane units.

LEP electrochemical properties

Cyclic voltammetry was used to investigate the electrochemical behaviors and estimate the highest occupied molecular orbital (HOMO) and lowest unoccupied molecular orbital (LUMO) LEP energy levels. The HOMO and LUMO levels of LEPs were calculated by comparison of the ferrocence value of −4.8 eV below the vacuum.[23,24] The LEP electrochemical properties are summarized in Table I. The cyclic voltammograms showed that oxidation onset potentials (E^{ox}_{onset}) were observed at about 1.01 and 0.85 eV for PFO and PFA, respectively. Moreover, the PFO and PFA optical band gaps (E_g's) determined from the absorption edge were 2.82 and 2.89 eV, respectively. The PFO and PFA electron affinities (LUMO level) were 2.98 and 2.76 eV, respectively, whereas the PFO and PFA ionization potential (HOMO level) levels were 5.81 and 5.65 eV. The electron-donor properties of diphenyl(*para*-toyl)amine led to a reduced PFA HOMO level compared to that of PFO.[25] Consequently, PFA possessed a lower HOMO level, which allowed an efficient hole injection from an ITO transparent anode. E^{ox}_{onset} values for PTFA1 and PTFA2 were observed at about 0.95 and 1.02 eV, respectively. PTFA1 and PTFA2 LUMO levels were 2.83 and 2.87 eV, respectively, whereas the HOMO levels were 5.75 and 5.82 eV, respectively. Higher LUMO and HOMO levels were obtained for PTFA2 in comparison with PTFA1; this was attributed to the reduced diphenyl(*para*-toyl)amine content. The PTOA electrochemical properties are also shown in Table I. PTOA exhibited lower LUMO and HOMO levels than the alkylfluorene copolymers, the PTFAs.

PL spectra of the LEPs

PL spectra of the LEPs in solution are shown in Figure 7. The maximum PL emission wavelengths and fwhm's in solution are summarized in Table II. The

TABLE I
Electrochemical Properties of the LEPs

Polymer	E_{ox} (eV)	UV–vis$_{onset}$ (nm)	E_g (eV)	HOMO (eV)	LUMO (eV)
PFO	1.01	440	2.82	5.80	2.98
PFA	0.85	430	2.89	5.65	2.76
PTFA1	0.95	425	2.92	5.75	2.83
PTFA2	1.02	420	2.95	5.82	2.87
PTOA	0.49	434	2.86	5.30	2.45

E_{ox}, onset potential; UV-vis$_{onset}$, onset of UV-vis absorption.

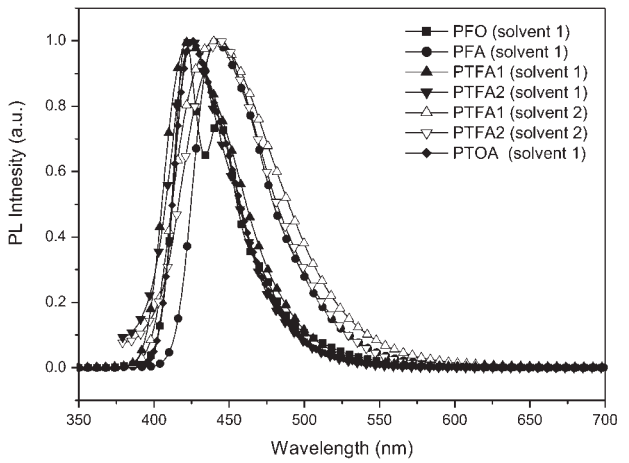

Figure 7 PL spectra of the LEPs in the solution state [filled symbols: solvent 1 (cyclohexanone); open symbols: solvent 2 (toluene)].

PL spectrum of PFO showed a maximum corresponding to the 0–0 transition at 421 nm with a well-defined vibronic feature (0–1 transition) at 442 nm.[25] The emission maximum of PL in solution for PFA was observed at 441 nm. The incorporation of the electron-donor moiety diphenyl(*para*-toyl)-amine onto the polymer backbone resulted in PL emission maximum redshifting compared to the homopolymer, PFO. On the other hand, the incorporation of the nonconjugated moiety tetraphenylsilane onto the polymer backbone of PFA resulted in the blueshifting of the PL emission maximum due to the reduced LEP conjugation length. The PTFA1 and PTFA2 results show PL emission maxima at 425 and 424 nm, respectively. The fwhm of PL also decreased with increasing tetraphenylsilane content. Furthermore, the solvatochromic effect resulted in the redshifting and broadening of the PL emission bands for PTFA1 and PTFA2 in toluene solution as compared to those in cyclohexanone. PTOA in cyclohexanone additionally showed PL with a maximum emission at 426 nm, which was attributed to the triarylaminooxadiazole group light-emitting unit.[21] The fwhm of the PTOA PL emission band was as narrow as the one emitting from the PTFA solution, despite the fact that the molecular interaction between the PTOA polymer chains was larger than that between the PTFA polymer chains.

The PL spectra of the LEPs in the solid film state are shown in Figure 8. The maximum PL emission wavelengths and fwhm's of PL in the solid film are summarized in Table II. PFO and PFA in the solid state showed broader emission bands than those in the solution state, which was associated with more energy levels of π–π* transition along the polymer backbone in the solid film state. The PL spectrum of PFO showed a maximum at 438 nm, with a well-defined vibronic feature at 464 nm and a shoulder at 493 nm. The longer shoulder wavelength was attributed to interchain excimer formation.[26,27] The maximum PL emission in the solid state for PFA was observed at 492 nm, a 51-nm redshift from PL in solution. The incorporation of adiphenyl(*para*-toyl)-amine into the polymer backbone would lead to emitter π–π stacking. A broad emission band was consequently observed in the 450–650 nm wavelength range for the PFA sample. The solvatochromic effect and excimer formed in the solid film were responsible for the redshifting and broadening of the PL emission band. Maximum PL emissions for PTFA1 and PTFA2 in the solid state were observed at 432 nm, a 60-nm blueshift from the PL of PFA. The incorporation of tetraphenylsilane groups would result in a reduced PFA conjugation length and, subsequently, the blueshifting of the PL emission band.

TABLE II
Film Thickness, PL, and EL Performance Values of the PLEDs

Device	LEP[a]	*d* (nm)[b]	λ_{max}^{PL} (nm)[c,e]	fwhm of PL (nm)[c]	λ_{max}^{PL} (nm)[d,e]	fwhm of PL (nm)[d]	λ_{max}^{EL} (nm)[f]	fwhm of EL (nm)	CIE (*x*, *y*) at 14 V[h]
I	PFO	53.0	421	43	438	51	436	47	(0.20, 0.21)
II	PFA	51.8	441	54	492	120	467	104	(0.18, 0.25)
III	PTFA1	53.8	425	56	433	57	442	95	(0.21, 0.22)
IV	PTFA2	50.7	424	48	432	52	434	75	(0.20, 0.18)
V	PTFA1	52.6	445	78	431	56	473	134	(0.25, 0.30)
VI	PTFA2	51.2	441	65	432	51	453	103	(0.24, 0.25)
VII	PTOA	71.0	426	45	453	81	454[g]	120[g]	(0.19, 0.26)[g]

[a] Devices I–IV and VII: the light-emitting layer coated with cyclohexanone solution; devices V and VI: the light-emitting layer coated with toluene solution.
[b] *d*, thickness of the light-emitting layer.
[c] PL from the LEP solution.
[d] PL from the solid film.
[e] λ_{max}^{PL}, the maximum PL emission wavelengths.
[f] λ_{max}^{EL}, the maximum EL emission wavelengths.
[g] Applied voltage = 18 V.
[h] CIE (*x*, *y*), Commission Internationale de L'Eclairage Coordinate.

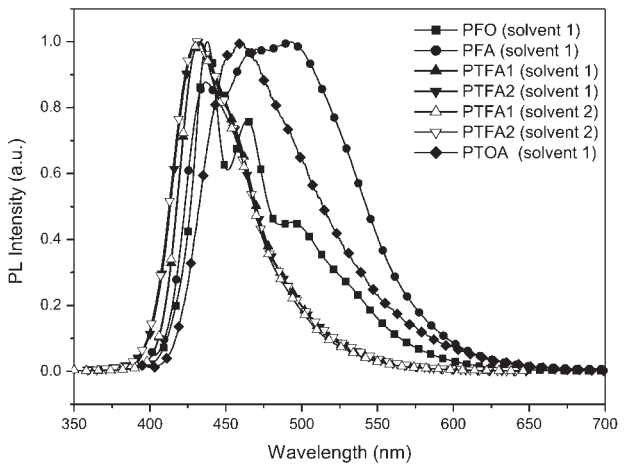

Figure 8 PL spectra of the LEP solid films [filled symbols: solvent 1 (cyclohexanone); open symbols: solvent 2 (toluene)].

Moreover, excimer emission was also completely suppressed with the incorporation of tetraphenylsilane groups onto the polymer backbone for the PTFA1 and PTFA2 samples. The fwhm of solid-film PL, therefore, was reduced significantly compared with those of PFO and PFA. Furthermore, the excimer suppression effect of the tetraphenylsilane moiety was further investigated by thermal annealing of the PTFA solid film coated with the cyclohexanone solution at elevated temperatures. The PL spectra of the PTFA1 and PTFA2 solid films were nearly the same after they were thermally treated at 120°C for 4 h. On the other hand, the PL emission bands of the PTFA1 and PTFA2 solid films coated with toluene solution were also nearly the same as the ones coated with cyclohexanone solution. The solvatochromic effect resulted in the blueshift of the PL emission bands of the PTFA solid film coated with toluene solution. Because of the blueshift, this PL emission band overlapped with the one coated with cyclohexanone solution. On the other hand, the PL emission maximum of the PTOA solid films was observed at 453 nm, with a large redshift (27 nm) from the PL in solution. The solvatochromic effect and excimer formed in the solid film were responsible for the PL emission band redshift and broadening because of strong interaction between the diphenyl(*para*-toyl)amine and oxadiazole groups.[21] This revealed that the tetraphenylsilane moiety excimer suppression effect was not effective for the PTOA sample consisting of strong electron-donating and electron-withdrawing moieties.

Optoelectronic properties of the LEP-based devices

PLED EL spectra

The EL spectra of the LEP-based devices under an applied voltage of 14 V are shown in Figure 9. The EL emission maximum wavelength, fwhm of EL, and Commission Internationale de L'Eclairage ($CIE_{x,y}$) coordinate values of the LEP-based devices are summarized in Table II. An EL emission band with a main peak at 436 nm, accompanied by two emission shoulders around 462 and 490 nm, was observed for the PFO-based device (device I). The EL spectrum of PFO resembled the PL spectrum closely. Moreover, the EL emission peak intensity at 438 nm decreased with the reduction of 9,9-dioctylfluorene content for the PFA-based device (device II), whereas the vibronic and excimer band emissions were enhanced with the incorporation of diphenyl(*para*-toyl)amine onto the polymer backbone compared to the PFO-based device. The EL emission maxima of PTFA1- and PTFA2-based devices (devices III and IV, coated with cyclohexanone) were observed at 442 and 434 nm, respectively. The incorporation of tetraphenylsilane groups resulted in a shortened PFA conjugation length and a blueshifted EL emission band. Excimer band emission was suppressed with the incorporation of tetraphenylsilane groups onto the PTFA2 polymer backbone. The fwhm's of EL for the PTFA-based devices were, therefore, reduced significantly compared to those of the PFA one. The EL emission color purities were enhanced because of the reduced fwhm's of EL for devices III and IV. However, the EL spectrum of device IV indicated that the bulky tetraphenylsilane moiety could not completely suppress excimer formation compared to that of the PFO-based device I. On the other hand, a strong solvatochromic effect of the EL spectra was observed for the PTFA1 and PTFA2 light-emitting layer devices coated with toluene solution. The poor solvent toluene resulted in polymer-chain aggregation in the solid film during the spin-coating process. The redshifting and broad-

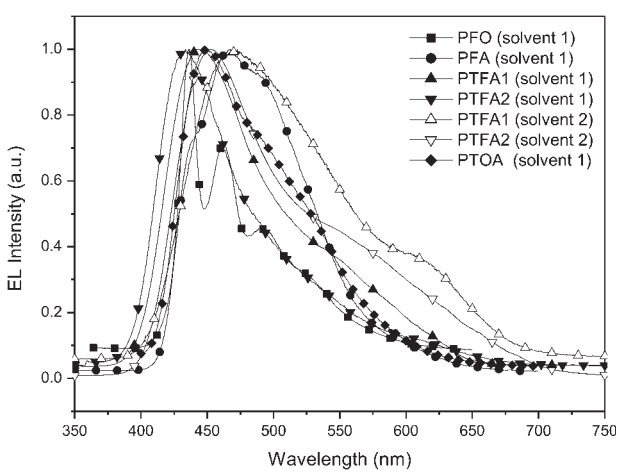

Figure 9 EL spectra of the LEP-based devices I–VI [filled symbols: solvent 1 (cyclohexanone); open symbols: solvent 2 (toluene)].

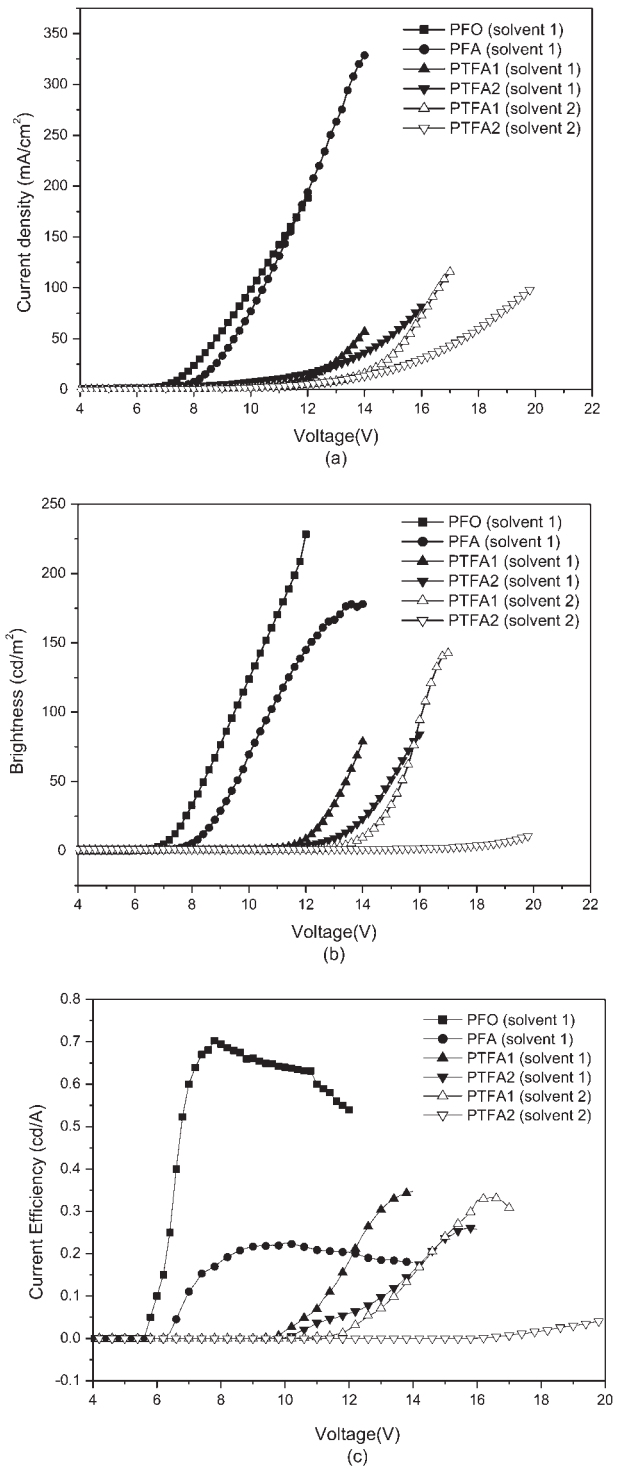

Figure 10 Current density, brightness, and current efficiency of the PLEDs [filled symbols: solvent 1 (cyclohexanone); open symbols: solvent 2 (toluene)].

ening of the EL emission band were observed for devices V and VI (coated with toluene) compared to devices III and IV. The EL emission color purities were also reduced because of the enhanced fwhm of EL for devices V and VI. Device VII (coated with PTOA) also showed a broader EL emission band than device IV. Light emission from the electromer $(M^+M^-)^*$ or electroplex $(M^+N^-)^*$ led to PTOA EL spectra broadening (475–650 nm), which corresponded to the interaction between oxadiazole (M) and diphenyl(4-tolyl)amine (N) groups in different polymer segments or chains.[21] This result demonstrates that the bulky tetraphenylsilane moiety could not effectively suppress electromer or electroplex formation for the PTOA-based device.

EL properties of the LEP-based devices

PLED current density, brightness, and current efficiency are shown in Figure 10. The current density of the PFA-based device was nearly the same as that of the PFO-based device. The enhanced effect of current density with the incorporation of the electron-donor moiety diphenyl(*para*-toyl)amine was diminished because of the reduced 9,9-dioctyl-fluorene content and shortened polymer backbone conjugation length. The reduction of emitter content led to a lower brightness and current efficiency for the PFA-based device compared to the one based on PFO. The turn-on voltage increased with increasing tetraphenylsilane content for the PTFA1 and PTFA2-based devices. Their current density and brightness were reduced compared to the PFO- and PFA-based devices. Moreover, the current efficiencies of the PTFA1- and PTFA2-based devices also decreased with decreasing emitter 9,9-dioctyl-fluorene content. In addition to emitter content, PLED EL was also affected by light-emitting layer morphology. Polymer film morphology was related to polymer-chain conformation in the solution state. Poor solvents, such as toluene, resulted in polymer-chain aggregation in the solid film during the spin-coating process. As a result, the carrier transporting capacity was reduced for the light-emitting layer. It is important to note that current density, brightness, and current efficiency of devices V and VI (coated with toluene) were, therefore, lower than those of the devices III and IV (coated with cyclohexanone) under the same applied voltage. Indeed, the EL performance of the PLEDs was determined by the conjugation structure and morphology of the LEP-based solid film.

CONCLUSIONS

Blue-light-emitting copolymers PTFA1 and PTFA2 containing 25 and 50 mol %, respectively, of tetraphenylsilane fluorophores were synthesized to study the bulky moiety effect on excimer suppression. The tetraphenylsilane with rigid bulky structure certainly suppressed aggregation and excimer formation among polymer-chain segments. The color purity of the alternating copolymer consisting of 9,9-dialkyl-

fluorene and diphenyl(*para*-toyl)amine was, therefore, improved. However, the EL spectra indicated that the bulky tetraphenylsilane moiety could not completely suppress excimer formation. Moreover, excimer formation was also closely related to the morphology of the light-emitting layer. The poor solvent toluene resulted in polymer-chain aggregation in the solid film during the spin-coating process. In this case, the formation of excimer could not be suppressed by the bulky moiety incorporation. Furthermore, electromers or electroplexes formed by the strong interaction between the electron-donating and electron-withdrawing moieties, such as oxadiazole and diphenyl(4-tolyl)amine groups, in different polymer segments or chains could not be prevented by the tetraphenylsilane moiety for the PTOA-based device. In conclusion, excimer and electromer suppression of the PLEDs were strongly dependent on the chemical structure of the LEP and the PLED fabrication conditions.

References

1. Kobayashi, H.; Kanbe, S.; Seki, S.; Kigchi, H.; Kimura, M.; Yudasaka, I.; Miyashita, S.; Shimoda, T.; Towns, C. R.; Burroughes, J. H.; Friend, R. H. Synth Met 2000, 111–112, 125.
2. Vaart, N. C. V. D.; Lifka, H.; Budzelaar, F. P. M.; Rubingh, J. E. J. M.; Hoppenbrouwers, J. J. L.; Dijksman, J. F.; Verbeek, R. G. F. A.; Woudenberg, R. V.; Vossen, F. J.; Hiddink, M. G. H.; Rosink, J. J. W. M.; Bernards, T. N. M.; Giraldo, A.; Young, N. D.; Fish, D. A.; Childs, M. J.; Steer, W. A.; Lee, D.; George, D. S. Society Information Display Symp 2004, 35, 1284.
3. Ranger, M.; Rondeau, D.; Leclerc, M. Macromolecules 1997, 30, 7686.
4. Bernius, M. T.; Inbasekaran, M.; O'Brien, J.; Wu, W. Adv Mater 2000, 12, 1737.
5. Fletcher, R. B.; Lidzey, D. G.; Bradley, D. D. C.; Walker, S.; Inbasekaran, M.; Woo, E. P. Synth Met 2000, 111–112, 151.
6. Neher, D. Macromol Rapid Commun 2001, 22, 1365.
7. Grimsdale, A. C.; Leclere, P.; Lazzaroni, R.; Mackenzie, J. D.; Murphy, C.; Setayesh, S.; Silva, C.; Friend, R. H.; Mullen, K. Adv Fun Matter 2002, 12, 729.
8. Sung, H. H.; Lin, H. C. Macromolecules 2004, 37, 7945.
9. Kreyenschmidt, M.; Klaerner, G.; Fuhrer, T.; Ashenhurst, J.; Karg, S.; Chen, W. D.; Lee, V. Y.; Scott, J. C.; Miller, R. D. Macromolecules 1998, 31, 1099.
10. Zeng, G.; Yu, W. L.; Chua, S. J.; Huang, W. Macromolecules 2002, 35, 6907.
11. Jacob, J.; Zhang, J.; Grimsdale, A. C.; Mullen, K.; Gaal, M.; List, E. J. W. Macromolecules 2003, 36, 8240.
12. Kulkarni, A. P.; Jenekhe, S. A. Macromolecules 2003, 36, 5285.
13. Xiao, S.; Nguyen, M.; Gong, X.; Cao, Y.; Wu, H.; Moses, D.; Heeger, A. J. Adv Fun Mater 2003, 13, 25.
14. Lin, W. J.; Chen, W. C.; Wu, W. C.; Niu, Y. H.; Jen, A. K. Y. Macromolecules 2004, 37, 2335.
15. Lee, J.; Cho, H. J.; Jung, B. J.; Cho, N. S.; Shim, H. K. Macromolecules 2004, 37, 8523.
16. Chou, C. H.; Hsu, S. L.; Dinakaran, K.; Chiu, M. Y.; Wei, K. H. Macromolecules 2005, 38, 745.
17. Liu, X. M.; He, C.; Hao, X. T.; Tan, L. W.; Li, Y.; Ong, K. S. Macromolecules 2004, 37, 5965.
18. Liu, X. M.; Xu, J.; Lu, X.; He, C. Org Lett 2005, 7, 2829.
19. Liu, X. M.; He, C.; Huang, J.; Xu, J. Chem Mater 2005, 17, 434.
20. Liu, X. M.; Xu, J.; Lu, X.; He, C. Macromolecules 2006, 39, 1397.
21. Lee, R. H.; Hsu, H. F.; Chan, L. H.; Chen, C. T. Polymer 2006, 47, 17001.
22. Pauling, L. The Nature of the Chemical Bond; 3rd ed.; Cornell University Press: Ithaca, NY, 1960.
23. Miller, L. L.; Nordblom, G. D.; Mayeda, E. A. J Org Chem 1972, 37, 916.
24. Yang, C. J.; Jenekhe, S. A. Macromolecules 1995, 28, 1180.
25. Palilis, L. C.; Lidzey, D. G.; Redecker, M.; Bradley, D. D. C.; Inbasekaran, M.; Woo, E. P.; Wu, W. W. Synth Met 2000, 111–112, 159.
26. Pei, Q.; Yang, Y. J Am Chem Soc 1996, 118, 7416.
27. Grice, A. W.; Bradley, D. D. C.; Bernius, M. T.; Inbasekaran, M.; Wu, W. W.; Woo E. P. Appl Phys Lett 1998, 73, 629.